

## Accounts

---

### Recent Progress in High-Resolution Spectroscopic Studies on Transient Molecules

Eizi Hirota

The Graduate University for Advanced Studies, 4259 Nagatsuta, Midori, Yokohama 226

(Received August 26, 1994)

The microwave and/or infrared spectra of alkali monoxides and  $\text{NO}_3$  were observed in order to characterize these molecules in detail, which play significant roles in atmospheric chemistry. Similar studies were carried out on a few inorganic molecules, including  $\text{Si}_n\text{H}_m$  neutrals and ions with  $n=1, 2$  and  $m=1, 2, 3$ , in view of their important roles in electronic-device processing. Recent innovations in high-resolution spectroscopic methods are briefly discussed.

Free radicals are defined as being molecular species that include (an) unpaired electron(s). Because chemical reactions proceed by breaking (a) chemical bond(s), followed by its (their) replacement by new one(s), free radicals exist as intermediates in chemical processes. As a result, they often act as the key species of chemical reactions. It is then natural to include in a discussion of free radicals some molecular species which do not have unpaired electrons, but are quite reactive and behave just like free radicals as intermediates in reaction processes. We refer to all such molecules as *transient molecules*. They are either difficult or impossible to isolate from other stable molecules, and can thus be investigated only *in situ* in systems where reactions are taking place.

Chemists have postulated the existence of appropriate intermediate species to explain the mechanisms of chemical reactions. In older days many of them were nothing but virtual existence. However, along with the advent of flash photolysis around 1950 and of lasers around 1960 the situation changed considerably; many important transient molecules have now been confirmed to really exist, and even their structures have been determined precisely, thanks to remarkable developments concerning spectroscopic methods. Lasers have improved the resolution and sensitivity of molecular spectroscopy by orders of magnitude.

Such spectroscopic investigations of transient molecules started in the visible and ultraviolet regions, where we expect to observe primarily the electronic transitions of molecules. It is certainly sensible to begin the study with electronic spectroscopy, because its high sensitiv-

ity is indispensable for the study of transient molecules, which are quite difficult to generate at high concentrations, and thus give only weak signals. In addition, electronic spectroscopy could be easily combined with a then new method of flash photolysis by the use of photographic plates. However, electronic spectroscopy has a few drawbacks: polyatomic molecules often predissociate in excited electronic states, prohibiting their high-resolution spectra from being recorded. It is more difficult to achieve high resolution with electronic spectroscopy than with spectroscopy in the long-wavelength regions, such as infrared and microwave spectroscopy. Fortunately, the sensitivity of these long-wavelength spectroscopic methods has recently been greatly improved and has reached a stage at which they could be successfully applied to quite a large number of transient molecules. The present paper illustrates a few examples of such studies recently carried out or being performed in the infrared and microwave regions.

High-resolution spectroscopic studies of transient molecules are highly rewarding for the following reasons:

**(1) Electronic Structure Unveiled through the Fine and Hyperfine Structure.** The angular momenta of an unpaired electron, orbital and/or spin, interact with other angular momenta in the molecule, such as the overall rotation, spin(s) of other unpaired electron(s) if any, and nuclear spin(s), splitting the rotational spectra and/or rotational structure into fine and/or hyperfine components. The unpaired electron(s) thus act(s) as a monitor by which we can obtain detailed information concerning the electronic structure

of the molecule.

**(2) Reaction Intermediates Traced in Real Time.** As already stressed, transient molecules act as intermediates in reaction processes. Therefore, their high-resolution spectra are ready to be used to follow the process of a reaction in detail. Since we can determine the distribution of such species even over an individual quantum state, the information can be extremely precious.

**(3) Applications to Astronomy.** It has been known that about half of the interstellar molecules so far detected are transient molecules under terrestrial or laboratory conditions. Once an interstellar molecule is identified, its high-resolution spectra serve as a monitor to diagnose atomic and molecular processes taking place in interstellar and circumstellar space.

**(4) Applications to Atmospheric Chemistry.** Artificial exhausts in the upper atmosphere of the Earth produced by human activities cause additional chemical reactions there, which can lead to a serious imbalance in the atmospheric compositions of the molecular species. Ozone depletion is the most famous example. The high-resolution spectra of transient molecules certainly provide us with clues of how to monitor minor, but crucial, species in the upper atmosphere.

**(5) Applications to Plasma Science and Related Fields.** A weak plasma with an electron density less than on the order of  $10^{12} \text{ cm}^{-3}$  is a good source for generating transient molecules. Hence, high-resolution spectroscopy of transient species occurring in a plasma provides us with a clue about how to diagnose the plasma conditions. We may find similar applications of high-resolution spectra to the diagnosis of molecular systems where chemical processes are taking place.

The examples we discuss in the present paper include alkali monoxides and the  $\text{NO}_3$  radical, both of which play important roles for atmospheric chemistry, as well as some inorganic molecules, such as  $\text{Si}_n\text{H}_m$ .

### Alkali Monoxides

Alkali monoxides,  $\text{MO}$  ( $\text{M}=\text{Li}, \text{Na}, \text{K}, \text{Rb}, \text{and Cs}$ ), have been attracting much interest for several reasons; three of them are mentioned below:

**(1) Ionic versus Neutral Potential Surfaces.** Several pieces of evidence, such as the hyperfine structure, as mentioned below, clearly indicate that alkali monoxides in the ground electronic states comprise almost completely ionized constituents,  $\text{M}^+$  and  $\text{O}^-$ . However, the ground states obviously dissociate into neutral fragments,  $\text{M}$  and  $\text{O}$ , because this dissociation limit is lowest in energy. For example, the ionization potential of  $\text{Na}$  is 5.138 eV, which surpasses the electron affinity of  $\text{O}$ , 2.103 eV.<sup>1)</sup> This situation is similar to that of alkali halides. There must thus be a crossing of the potential curves somewhere between the equilibrium bond length of the lowest bound state and the dissociation limit. Nemukhin, Almlöf, and Heiberg<sup>2)</sup>

calculated the potential-energy curves of the three lowest-lying electronic states ( $^2\Sigma^+$ ,  $^2\Pi$ , and  $^2\Sigma^-$ ) of  $\text{LiO}$  by using a complete active space self-consistent field (CASSCF) method; however, they did not pay attention to the crossing or avoided crossing. Woodward, Hayden, and Gole<sup>3)</sup> have recently observed the emission spectra of alkali monoxides prepared by the reaction of alkali metals with dinitrogen monoxide; the emission extended from 450 to 570 nm in the case of  $\text{LiO}$ , and was assigned to the  $\text{B}^2\Pi \rightarrow \text{X}^2\Pi$  transition. The upper  $\text{B}^2\Pi$  state is located at about 3.0 eV above the ground state, and the chemical bond in this state is supposed to be of covalent nature; thus, the B state may correspond to the covalent counterpart.

**(2) Symmetry of the Ground Electronic State,  $^2\Pi$  versus  $^2\Sigma^+$ .** It has been shown both experimentally<sup>4–10)</sup> and theoretically<sup>2,11–17)</sup> that the ground states of  $\text{LiO}$  and  $\text{NaO}$  belong to  $^2\Pi$ , whereas those of  $\text{RbO}$  and  $\text{CsO}$  belong to  $^2\Sigma^+$ . A similar crossover of symmetry has been known for a few series of molecules. A most typical example is the  $\text{C}_{2n}\text{H}$  series ( $n$  denoting an integer). The first member of this series,  $\text{CCH}$ , has a  $^2\Sigma^+$  ground state accompanied by a  $^2\Pi$  excited state at about  $3600 \text{ cm}^{-1}$  above the ground state.<sup>18)</sup> Although the  $^2\Sigma$  state is also lowest in energy in the second molecule,  $\text{CCCCH}$ ,<sup>19)</sup> there are some anomalous features in the rotational spectra of this molecule, particularly in those in excited bending states, indicating the presence of a low-lying  $^2\Pi$  state.<sup>20)</sup> The  $^2\Pi$  state becomes the ground state in the third molecule,  $\text{CCC-CCCH}$ . It took some time for Saito et al. to realize that the interstellar spectra already observed were to be assigned to this molecule;<sup>21,22)</sup> they initially thought the  $\text{C}_6\text{H}$  molecule has a  $^2\Sigma^+$  ground state, and searched for its spectra at even multiples of an estimated  $B$  rotational constant, but did not scan the region around odd multiples of the  $B$  constant, where the rotational lines of a  $^2\Pi$  linear molecule were expected to appear. Another example is the series  $\text{CN}$ ,  $\text{SiN}$ , and  $\text{GeN}$ ; it has been known that the first two have  $^2\Sigma^+$  ground states and that the lowest excited state of  $^2\Pi$  symmetry is located at  $9122.042\,66\,(30)$  [ $v=0$ ]<sup>23)</sup> and  $1972.759\,53\,(56)$  [ $T_{00}$ ]<sup>24)</sup>  $\text{cm}^{-1}$  above the ground state for  $\text{CN}$  and  $\text{SiN}$ , respectively. Although it has not been shown experimentally,  $\text{GeN}$  is very likely to be a  $^2\Pi$  molecule in the ground electronic state.

As mentioned above, since alkali monoxides are almost completely ionic, an unpaired electron, or more appropriately stated, a positive hole, is localized on the oxygen atom. This hole may occupy either a  $p\pi$  or  $p\sigma$  orbital, resulting in a  $^2\Pi$  or  $^2\Sigma^+$  state, respectively. Allison et al.<sup>14,15)</sup> have explained the energy difference between the  $^2\Pi$  and  $^2\Sigma^+$  states in terms of two competing factors: the quadrupole attraction of the oxygen ion, which favors  $^2\Pi$  states, and of the Pauli repulsion, which favors  $^2\Sigma^+$ . Most interesting is the case of  $\text{KO}$ , for which the two states,  $^2\Pi$  and  $^2\Sigma^+$ , are expected to

be very close to each other. In fact, conflicting results, both in experiment<sup>4,6)</sup> and *ab initio* calculation,<sup>14–17,25)</sup> have been reported for KO.

**(3) Origin of the Sodium Night Glow and of the Luminescence of Meteor Trails.** Chapman<sup>26)</sup> ascribed the sodium D-line emission in the mesosphere to sodium atoms in the  $^2P$  excited state prepared by the reaction of NaO and O. However, Plane and Husain<sup>27)</sup> have found that this reaction, if NaO was in the  $^2\Pi$  state, produced a too-small amount of excited sodium atoms to account for the emission. Herschbach et al.<sup>28)</sup> have recently pointed out that the reaction of Na with ozone resulted in a considerable amount of NaO in the  $A^2\Sigma^+$  state, which, when reacted with O, produced sodium atoms in  $^2P$  with a branching ratio as large as 2/3.

In order to clarify the various points mentioned above, including the mechanism for the sodium D emission in the mesosphere, more information is obviously indispensable concerning alkali monoxides and their related molecules in low-lying electronic states. Yamada and his collaborators have thus applied microwave and infrared diode laser spectroscopy to alkali monoxides; their so-far obtained results are summarized below.

**LiO.** Yamada et al.<sup>8)</sup> observed the rotational spectrum and Yamada and Hirota<sup>9)</sup> the fundamental vibrational band of LiO. Both of these studies confirmed that the ground electronic state of LiO is  $^2\Pi$ , as reported in previous investigations. The observed  $A$ -type doubling constants, when interpreted based on some assumptions, lead to a separation between the lowest excited  $A^2\Sigma^+$  state and the ground  $X^2\Pi$  state to be 2000 to 2500  $\text{cm}^{-1}$ . The fundamental frequency, harmonic frequency, and vibrational anharmonicity have been determined to be:

$$\nu_0 = 799.067\ 11\ (29)\ \text{cm}^{-1},$$

$$\omega_e = 814.62\ (15)\ \text{cm}^{-1},$$

and

$$\omega_e x_e = 7.78\ (15)\ \text{cm}^{-1},$$

where the values in parentheses denote the standard deviations. [This statement holds throughout the present paper, unless otherwise commented.] The equilibrium internuclear distance is calculated from the  $B_e$  constant to be

$$r_e = 1.688\ 221\ 59\ (2)\ \text{\AA}.$$

The axially symmetric component of the nuclear quadrupole coupling constant ( $eQq_0$ ) of  $^7\text{Li}$  was determined to be 0.463 (20) MHz in the ground vibronic state, which may be compared with the corresponding value [0.420 792 (34) MHz] of LiF.<sup>29)</sup> The latter molecule has been known to be a most typical ionic molecule, and, thus, this comparison of the nuclear quadrupole coupling constants indicates that LiO is also an ionic molecule. Four magnetic hyperfine coupling

constants ( $a$ ,  $b$ ,  $c$ , and  $d$ ) have been determined; the magnitudes of these constants are quite small, reflecting the fact that the unpaired electron or the hole is primarily localized in the oxygen ion. The Fermi interaction constant ( $b_\eta$ ) is negative (−17.77 MHz); the negative sign is ascribed to spin polarization.

**NaO.** Yamada et al.<sup>7)</sup> have observed the rotational spectrum in order to determine the molecular parameters in the ground ( $v=0$ ) and three excited ( $v=1$  to 3) vibrational states. As in the case of LiO, the ground electronic state was confirmed to be  $^2\Pi$ . A simple interpretation of the observed  $A$ -type doubling constants allowed Yamada et al. to estimate the  $A^2\Sigma^+ - X^2\Pi$  separation to be about 2050  $\text{cm}^{-1}$ . They calculated the harmonic vibrational frequency by inserting the observed  $B_e$  and  $D_e$  constants in the following expression:

$$\omega_e = (4B_e^3/D_e)^{1/2} = 492.27\ \text{cm}^{-1},$$

and the equilibrium internuclear distance  $r_e$  from  $B_e$  to be

$$r_e = 2.051\ 548\ (1)\ \text{\AA}.$$

The nuclear quadrupole coupling constant is −6.81 (21) MHz, which may be compared with the typical “ionic” value (−8.4980 MHz) of NaF.<sup>30)</sup> The Fermi interaction constant is again negative (−5.14 MHz) due to the effect of spin polarization.

**KO.** As mentioned earlier, the two lowest electronic states ( $^2\Pi$  and  $^2\Sigma^+$ ) are closest to each other for this molecule. In fact, Yamada et al.<sup>31)</sup> have observed the rotational spectra in both a  $\Pi$  and  $\Sigma$  state. They fitted the observed spectra to a  $2 \times 2$  matrix, of which the off-diagonal block consists of a spin-orbit term [the interaction constant ( $A_{SO}$ ) was fixed to −104  $\text{cm}^{-1}$ ] and an electronic Coriolis term. The fitting was far from satisfactory, particularly for high- $N$  lines of the  $^2\Sigma^+$  state; the poor fitting of the  $^2\Sigma^+$  lines may be accounted for by interactions of the  $v=0$  level of this electronic state with the  $v=1$  level of the  $^2\Pi$  state. Nevertheless, Yamada et al. have demonstrated that the  $^2\Sigma^+$  state is higher than the  $^2\Pi$  state by about 200  $\text{cm}^{-1}$ . The rotational constant was determined to be 8272.5 and 9486.5 MHz for the  $^2\Pi$  and  $^2\Sigma^+$  states, respectively, from which the internuclear distance was calculated to be 2.3211 and 2.1675  $\text{\AA}$ , respectively. Unfortunately, the analysis of the observed spectra did not yield reliable centrifugal distortion constants, and thus only a rough estimate could be made for the vibrational frequencies to be 300 to 400  $\text{cm}^{-1}$ .

**RbO.** Yamada and Hirota<sup>32)</sup> have observed three sets of the rotational spectra which, in agreement with the results of previous studies, conformed with those of a  $^2\Sigma$  molecule. The most dominant set was assigned to  $^{85}\text{RbO}$  in the ground vibrational state; the hyperfine structure was consistent with a nuclear spin of 5/2. The second set was nicely explained by an isotopic species,  $^{87}\text{RbO}$ , present in natural abundance (about 1/3 as

abundant as  $^{85}\text{RbO}$ ); the observed hyperfine structure indicated the spin to be  $3/2$ . The last set was assigned to  $^{85}\text{RbO}$  in the first excited vibrational state.

The spin-rotation interaction constant ( $\gamma$ ) was determined to be  $-1072.556$  (35) and  $-1068.20$  (11) MHz for  $^{85}\text{RbO}$  and  $^{87}\text{RbO}$ , respectively. When the spin-orbit interaction constant ( $A_{\text{SO}}$ ) was assumed to be  $-100\text{ cm}^{-1}$ , the  $\gamma$  constants led to an excitation energy ( $E_{\Pi} - E_{\Sigma}$ ) of  $2745\text{ cm}^{-1}$ . This value probably represents an upper bound, in view of the assumptions involved. It should be noted that, although the spectra of  $^{85}\text{RbO}$  in  $v=1$  and of  $^{87}\text{RbO}$  in  $v=0$  were observed, we could not observe the spectra in the  $\Pi$  electronic state. Because the cell temperature was about  $500$  to  $550\text{ }^{\circ}\text{C}$ , this fact indicates the  $\Pi$  state is higher than the  $\Sigma$  ground state by at least  $500\text{ cm}^{-1}$ .

The three  $B$  rotational constants were analyzed by assuming the following reduced-mass ( $\mu$ ) dependences of  $B_e$  and  $\alpha^B$ :

$$B_e = h/[8\pi^2 \mu r_e^2]$$

and

$$\alpha^B = \mu^{-3/2} [\alpha_{\text{red}}].$$

The interatomic distance ( $r_e$ ) calculated from the thus-obtained equilibrium rotational constant ( $B_e$ ) is  $2.254\,194\,0$  (11) Å. The  $B_e$  constant of  $^{85}\text{RbO}$  was combined with the centrifugal distortion constant of the same isotopic species extrapolated to the equilibrium in order to estimate the harmonic vibrational frequency to be  $387.91$  (10)  $\text{cm}^{-1}$ .

The nuclear quadrupole coupling constant of  $^{85}\text{RbO}$  in the ground vibrational state was determined to be  $-28.1$  (2.5) MHz. A comparison of this value with the value of  $\text{RbF}$  [ $-70.341\,5$  (22) MHz<sup>33)</sup>] for example, which has been known as a most typical example of ionic molecules, shows that  $\text{RbO}$  is also an ionic molecule. The magnetic hyperfine structure parameters [ $b=605.4$  (40) and  $c=162$  (11) MHz] obtained for  $^{87}\text{RbO}$  in the ground vibronic state are in fair agreement with the values [417 and 143 MHz] of a previous ESR study.<sup>6)</sup> The Fermi interaction constant, when compared with the atomic value, leads to an  $s$ -character of the unpaired electron orbital to be about 18.7%.

**CsO.** Yamada and Hirota<sup>32)</sup> have observed the rotational spectra of  $\text{CsO}$  in ground and excited vibrational states up to  $v=3$ , which were again consistent with the ground electronic state being a  $^2\Sigma^+$  state. A positive spin-rotation interaction constant gave a somewhat better fitting of the observed spectrum than a negative one, although the difference between the two was minor. The positive spin-rotation interaction constant is rather difficult to explain on the basis of a simple  $\Pi$  and  $\Sigma$  two electronic-states model; we need to take into account higher excited electronic states as well. Unfortunately, not much information has been available for such states. The expression  $4AB/(E_{\Pi} - E_{\Sigma})$  for the spin-rotation interaction constant with  $A=100\text{ cm}^{-1}$  gives the  $\Pi - \Sigma$

energy difference to be  $6170\text{ cm}^{-1}$ , which represents an upper bound for the excitation energy of the lowest excited electronic state. The observed spin-rotation interaction constants show a quite large vibrational-state dependence:  $432.275$  (47),  $371.62$  (14),  $286.00$  (16), and  $144.65$  (13) MHz for  $v=0$  to 3, respectively. This  $v$  dependence will be useful in refining the vibronic interaction model.

The  $B$  rotational constant extrapolated to the equilibrium leads to an interatomic distance ( $r_e$ ) of  $2.300\,744$  (16) Å. The  $B_e$  and  $D_e$  constants give a harmonic frequency ( $\omega_e$ ) of  $356.80$  (7)  $\text{cm}^{-1}$ .

The nuclear quadrupole coupling constant is again quite small [ $-24.9$  (3.1) MHz in  $v=0$ ], which may be compared with the corresponding value of  $\text{CsF}$  [ $1.245\,6$  (28) MHz<sup>34)</sup>]. Two hyperfine parameters [ $b=426.42$  (35) and  $c=118.06$  (64) MHz] obtained for the ground vibronic state are in fair agreement with an ESR result [351 and 118 MHz,<sup>6)</sup> respectively]. A Fermi interaction constant of  $465.8$  MHz leads to a rough estimate of the  $s$ -character (18.9%) for the unpaired electron orbital.

### Nitrate Radical $\text{NO}_3$

**Introductory Remarks.** Among the so-called  $\text{NO}_x$  (more precisely speaking,  $\text{NO}_y$ ) molecules, two have been most incompletely characterized; they are  $\text{NO}_3$  and  $\text{N}_2\text{O}_5$ . Both of them play substantial roles in the chemical processes in the upper atmosphere of the Earth, as summarized by Wayne et al.<sup>35)</sup> The nitrate radical  $\text{NO}_3$  is more interesting than  $\text{N}_2\text{O}_5$  from a molecular structure point of view; it is probably a planar symmetric-top free radical in a doublet state, which is quite rare.

It has been known for a long time that the nitrate radical absorbs strongly in the visible region; it was in 1983 that the radical was subjected to laser spectroscopic investigations for the first time. Ishiwata et al.<sup>36)</sup> and Nelson et al.<sup>37)</sup> observed laser-induced fluorescence (LIF) and dispersed fluorescence of the visible bands. Although both of the two groups partly resolved the vibrational structure, they arrived at different conclusions concerning the geometry of the radical in the ground electronic state; Ishiwata et al. interpreted their data based on  $D_{3h}$  symmetry, whereas Nelson et al. preferred  $C_{2v}$  to  $D_{3h}$ . Because no rotational structure was resolved in either of these studies, the geometry of the radical has not been established. Kim et al.<sup>38)</sup> have recently recorded dispersed fluorescence and have tried to reconcile two views,  $D_{3h}$  versus  $C_{2v}$ , by stating that the vibrational motions average over the three local  $C_{2v}$  structures to give the  $D_{3h}$  structure. More recently, two groups have recorded the LIF spectra of  $\text{NO}_3$  prepared in a molecular beam.<sup>39,40)</sup> Although the observed spectra were resolved into many rotational lines, they were too complicated to be analyzed.

Walsh<sup>41)</sup> discussed the electronic structure and shape of the  $\text{NO}_3$  radical on a basis of a molecular-orbital

consideration. He gave the electronic configuration of the ground state as being

$$\cdots(e')^4(e'')^4(a_2')^1 \quad \tilde{X}^2A_2',$$

where the three highest-occupied molecular orbitals (HOMO) are all derived from combinations of essentially nonbonding atomic orbitals localized on the oxygen atoms. The N–O bonding orbitals, which are much lower in energy than the nonbonding orbitals mentioned above, definitely favor a planar structure, whereas other occupied orbitals, including the three mentioned above, do not show much preference. Walsh thus concluded the NO<sub>3</sub> molecule to be planar. He interpreted the strong visible absorption to be caused by a transition from the ground  $\tilde{X}^2A_2'$  state to the  $\tilde{B}^2E'$  state, whose electronic configuration is expressed as

$$\cdots(e')^3(e'')^4(a_2')^2 \quad \tilde{B}^2E'.$$

We may then expect that there is another excited electronic state with the

$$\cdots(e')^4(e'')^3(a_2')^2 \quad \tilde{A}^2E''$$

electronic configuration between the ground state and the  $\tilde{B}$  state. [We renamed the excited state associated with the visible absorption as  $\tilde{B}$  rather than  $\tilde{A}$ , as called by Walsh, because the  $E''$  state is certainly lower in energy than the  $E'$  state.] It should be noted that the transition between the ground and the  $\tilde{A}$  states is electronically forbidden, and thus no spectroscopic data were available concerning the  $\tilde{A}$  state. Weaver et al.<sup>42)</sup> have applied photodetachment spectroscopy to the NO<sub>3</sub><sup>−</sup> ion and have located the  $\tilde{A}$  state at  $7001 \pm 105$  cm<sup>−1</sup> above the ground state. They also observed two progressions, one in  $\nu_1$  and the other in  $\nu_4$ . The appearance of the latter progression was somewhat surprising, because the  $\nu_4$  vibration belongs to  $E'$  symmetry. Weaver et al. explained this observation by a vibronic interaction of the ground state with the  $\tilde{B}^2E'$  state.

A number of *ab initio* calculations have been carried out.<sup>43–52)</sup> Most of these studies have focussed on the geometry of the molecule in the ground electronic state; although some of them favor a  $D_{3h}$  structure, whereas others prefer  $C_{2v}$  to  $D_{3h}$ , all of the calculations have agreed in that the energy difference between the two forms is quite small. The  $C_{2v}$  structure means the geometry where one of the N–O bonds is longer than the other two.

In view of the importance of the nitrate free radical in atmospheric chemistry and many related fields, Ishiwata, Kawaguchi, and their collaborators have carried out a systematic study of NO<sub>3</sub>, mainly using infrared diode-laser and infrared Fourier-transform spectroscopy in order to clarify its molecular as well as electronic structure in detail.

**The  $\nu_3$  and Other Infrared Bands. Vibronic Interaction between the  $\nu_3$  State in the Ground**

**State Manifold and Excited Electronic States of  $E'$  Symmetry.** Ishiwata et al.<sup>53)</sup> and Kawaguchi et al.<sup>54)</sup> have observed a band at around 1492 cm<sup>−1</sup> using infrared diode lasers as sources. These studies resolved the rotational structure of NO<sub>3</sub> for the first time. They assigned this band to a vibrational band of NO<sub>3</sub> in its ground electronic state. By taking ground-state combination differences they showed that the lower state, namely the ground vibronic state, conformed perfectly with a regular triangle geometry; only  $K''=3n$  ( $n$  denoting an integer) and, for  $K''=0$ , only odd  $N$  rotational levels were found to be present. The molecular parameters that they derived from the observed spectrum are:

$B$	0.458 575 (22)	
$D_N \times 10^5$	0.125 6 (49)	[0.131]
$D_{NK} \times 10^5$	−0.237 (11)	[−0.244]
$\epsilon_{bb}$	−0.016 25 (30)	

in cm<sup>−1</sup>, where  $C=B/2$  and  $D_K=-(2D_N+3D_{NK})/4$  were assumed. The values in square brackets denote those obtained from an appropriate force field; the observed values agree quite well with these. The observed spin-rotation splittings were accounted for by taking into account only the  $\epsilon_{bb}$  term, in agreement with the expectation based on the electronic structure (as discussed above). The  $\epsilon_{bb}$  term receives contributions from interactions with excited electronic states of  $E''$  symmetry, because the  $b$  or  $a$  components of the electronic orbital angular momentum belong to  $E''$  symmetry. When the spin-orbit interaction constant of oxygen (150 cm<sup>−1</sup>) is used together with a pure precession hypothesis, we arrive at an estimated value of  $-0.039$  cm<sup>−1</sup> for  $\epsilon_{bb}$ , where only the  $\tilde{A}^2E''$  state is considered to be the excited state. This value is of the same order of magnitude as the observed constant.

In contrast with the lower, i.e. ground, state, Ishiwata et al. and Kawaguchi et al. noticed a few anomalies present in the upper state of the transition; some of the anomalies could not be explained if the transition was purely vibrational. These anomalies are listed below:

(1) A small spin-orbit interaction term necessary to explain the spin doubling.

The  $\epsilon_{bb}$  term was found to be insufficient to explain all of the spin doublings in the upper state. The observed splittings could be reproduced only when a small spin-orbit term was introduced. The effective coupling constant was

$$a_{\text{eff}} |<L_z>| = 0.173\,29\, (47) \text{ cm}^{-1}.$$

We may understand the presence of such a spin-orbit interaction term by a mixing of this upper state with excited electronic states of  $E'$  symmetry; the upper state belongs to  $E'$  vibronic symmetry.

The vibronic Hamiltonian may be written in the following way:<sup>55)</sup>

$$H'/hc = V_1 q \{ \exp[i(\theta - \alpha)] + \exp[-i(\theta - \alpha)] \} \\ + V_2 q^2 \{ \exp[i(\theta + 2\alpha)] + \exp[-i(\theta + 2\alpha)] \} + \dots, \quad (1)$$

where  $\theta$  denotes the azimuthal angle of the unpaired electron and  $q \exp(\pm i\alpha)$  represents the degenerate vibrational coordinates ( $q_3$  in the present example). We refer to the first term in  $V_1$  as the first-order vibronic interaction term and the second term in  $V_2$  as the second-order vibronic interaction term. The mixing that we are considering occurs primarily through the first-order term; the effective spin-orbit interaction constant is given by

$$a_{\text{eff}} = [|h_1| / \Delta E]^2 A_{\text{SO}}, \quad (2)$$

where  $h_1$  denotes the matrix element of the first-order term between the  $\nu_3$  state and an excited state of  $E'$  symmetry, the  $\bar{B}$  state being a most typical example;  $\Delta E$  stands for the excitation energy of the  $E'$  electronic state. When  $\Delta E$  is taken to be  $15000 \text{ cm}^{-1}$  and  $A_{\text{SO}}$  to be  $30 \text{ cm}^{-1}$ , the observed value of  $a_{\text{eff}}$  is reproduced by setting  $|h_1| = 1139 \text{ cm}^{-1}$ .

This first-order vibronic term also reduces the harmonic frequency of the  $\nu_3$  mode by  $2|h_1|^2/\Delta E$ , which is equal to  $173 \text{ cm}^{-1}$ , to be compared with the observed frequency of  $1492 \text{ cm}^{-1}$ .

(2) Observed levels of  $K'=7$  and  $K'=10$  shifted downward and upward, respectively, and the shifts increased with the  $N$  values involved.

This perturbation could be explained by a Coriolis interaction of the  $\nu_3$  state with the  $E''$  component of the  $\nu_2 + 2\nu_4$  state.<sup>54)</sup> Namely the  $k, l = \pm 8, \pm 2$  and  $\pm 11, \pm 2$  levels of the latter vibrational state interact with the  $k, l = \pm 7, \pm 1$  and  $\pm 10, \pm 1$ , respectively, to shift the latter levels downward and upward, respectively, as observed. Although the Coriolis interaction constant ( $\xi$ )-[the coefficient of  $\{N(N+1) - k(k \pm 1)\}^{\frac{1}{2}}$  in the interaction matrix] is as small as  $0.00197 (94) \text{ cm}^{-1}$ , the analysis allowed Kawaguchi et al.<sup>54)</sup> to locate the perturbing level ( $\nu_2 + 2\nu_4$ ) at  $1492 + 9 = 1501 \pm 1 \text{ cm}^{-1}$ . This term value may be favorably compared with the sum  $1520 \text{ cm}^{-1}$  of the  $\nu_2$  ( $762 \text{ cm}^{-1}$ )<sup>56)</sup> and  $2\nu_4$  ( $758 \text{ cm}^{-1}$ )<sup>42)</sup> frequencies.

(3) Discrepancy between the observed and calculated first-order Coriolis coupling constants.

The first-order Coriolis coupling term ( $C\zeta$ ) was determined to be  $0.044277 (26) \text{ cm}^{-1}$ , which, when divided by  $C$ , led to a  $\zeta$  of about 0.19. This value differs greatly from the  $\zeta$  value of 0.7, calculated using an appropriate force field.

In an ordinary symmetric-top molecule, the azimuthal motion of a degenerate mode is "free" rotation. In fact, the azimuthal part of the wavefunction of a degenerate vibration is expressed as  $(2\pi)^{-\frac{1}{2}} \exp[i l \alpha]$ , where  $l$  denotes an integer, the absolute value of which is equal to  $v, v-2, \dots, 1$  or 0 ( $v$  means the vibrational quantum number of the degenerate mode). When vibronic coupling between the  $\nu_3$  state and excited elec-

tronic states of  $E'$  symmetry is taken into account, the azimuthal motion is no longer free, but is hindered by a three-fold trough in the potential. This fact can be demonstrated by using the vibronic Hamiltonian Eq. 1; it may be used to derive an effective potential function for the  $\nu_3$  mode, as follows:<sup>55)</sup>

$$V_{\text{eff}} = (\omega/2)q^2 - (|h_1|^2/\Delta E)q^2 - (|h_1 h_2|/\Delta E)(q_+^3 + q_-^3) + \dots, \quad (3)$$

where the first term in the right-hand side denotes the harmonic potential, the second term the correction for the harmonic frequency already mentioned, and the third term represents a three-fold barrier hindering the azimuthal motion. A simple perturbation calculation shows that this term really reduces the average of the vibrational angular momentum by the following factor:

$$\langle p_\alpha \rangle = 1 - 48[|h_1 h_2| / (\omega \Delta E)]^2. \quad (4)$$

In the above equations  $h_2$  stands for the matrix element of the second-order term in the vibronic Hamiltonian. The observed  $\zeta$  constant is reproduced when  $|h_1 h_2|/\Delta E$  is equal to  $185 \text{ cm}^{-1}$ .

(4)  $K'=1$  spin-rotation splittings required to introduce an anisotropy term ( $\epsilon_{bb} - \epsilon_{aa}$ ) of  $-0.00242 (42) \text{ cm}^{-1}$ , as compared with  $\epsilon_{bb} = -0.015326 (33) \text{ cm}^{-1}$ . A vibration-rotation interaction term of  $(\Delta l, \Delta K) = (2, -4)$ , needed with a coefficient two to three orders of magnitude larger than those in other ordinary molecules of the same size, such as  $\text{CHF}_3$ .

Both of these observations seem to indicate that the  $\text{NO}_3$  molecule tends to deviate from  $D_{3h}$  symmetry. They can be explained by higher-order perturbations involving vibronic terms, as shown by Hirota et al.<sup>55)</sup>

(5) Five infrared bands observed in the regions from  $1500$  up to  $2600 \text{ cm}^{-1}$ .

Kawaguchi et al.<sup>57,58)</sup> have observed these bands mainly by an infrared Fourier-transform spectrometer. They have found that the lower states of these bands were identical to the ground vibronic state and the upper states were all of  $E'$  symmetry. They have also noticed that these bands were not much weaker than the  $\nu_3$  fundamental band; the relative intensities of the observed bands are:

assignment	band origin/ $\text{cm}^{-1}$	intensity
$\nu_2$	762	0.8
$\nu_3$	1492	4.7
?	1927	3.0
$5\nu_4$	2024	1.5
$\nu_1 + 3\nu_4$	2155	2.0
$\nu_1 + \nu_3$	2518	2.1
$2\nu_1 + \nu_4$	2585	1.7

In the above the data concerning the  $\nu_2$  band are cited from a paper by Friedl and Sander,<sup>56)</sup> who also reported on an observation of the  $\nu_3$  band in agreement with Kawaguchi et al.<sup>53,54)</sup> These observations are all indicative of strong vibronic interactions between the  $E'$  vibrational levels in the ground electronic-state manifold

and excited electronic states of  $E'$  symmetry; these perpendicular bands borrow intensities from the electronic transition  $\tilde{B}^2E' \leftarrow \tilde{X}^2A'_2$ . A vibronic interaction often causes negative anharmonicity for the modes involved in the interaction. This applies to the  $\nu_4$  mode, particularly in the present case; observations of higher overtones, such as the  $5\nu_4$  mode, were made possible by the strong vibronic interaction; the  $5\nu_4$  band appeared at  $2024\text{ cm}^{-1}$ , which was larger than five times the fundamental frequency ( $363\text{ cm}^{-1}$ ), i.e.  $1815\text{ cm}^{-1}$ .

It should be added that quite recently Mayer et al.<sup>59)</sup> extended the vibronic interaction model discussed above by introducing two vibrational modes ( $\nu_3$  and  $\nu_4$ ) simultaneously. However, the results that they obtained remain essentially the same as those described above.

**Observation of  $\tilde{A} \leftarrow \tilde{X}$  Vibronic Bands; Vibronic Interactions within the  $\tilde{A}^2E''$  Excited State.**

In order to understand the  $\text{NO}_3$  radical in more detail, Ishiwata et al.<sup>60)</sup> have been observing the  $\tilde{A}^2E'' \leftarrow \tilde{X}^2A'_2$  transition using a near-infrared diode-laser spectrometer. They have scanned the region from  $7350$  to  $7600\text{ cm}^{-1}$  and have detected a number of weak lines. As mentioned earlier, since the  $\tilde{A} \leftarrow \tilde{X}$  transition is electronically forbidden, the weak lines that Ishiwata et al. have observed must be ascribed to (a) vibronic band(s). Because Weaver et al.<sup>42)</sup> have located the  $\tilde{A}^2E''$  state at  $7001 \pm 105\text{ cm}^{-1}$ , the excited vibrational mode is possibly either  $\nu_2$  or  $\nu_4$ . According to Walsh,<sup>41)</sup> it is reasonable to assume that the  $\text{NO}_3$  radical is also planar in the  $\tilde{A}$  state, and, thus, the vibronic state with  $\nu_2$  or  $\nu_4$  excited belongs to  $E'$  or  $A'_1 + A'_2 + E''$  symmetry, of which  $E'$  and  $A'_1$  are vibronically accessible from the ground vibronic state. Three doublet series have been identified among the observed lines; the patterns of these series seem to conform to those of a parallel band, indicating that the  $\nu_4$  mode is excited in the upper state of the transition. In order to aid the spectral analysis, the  $A'_1$  and  $A'_2$  vibronic states were examined by paying special attention to the rotational structure in these states.<sup>61)</sup>

The two components of the electronic wavefunction for the  $\tilde{A}^2E''$  state are expressed as  $|+\rangle$  and  $|-\rangle$ , and those of the  $\nu_4$  vibrational wavefunction as  $|l+\rangle$  and  $|l-\rangle$ . Then, the three vibronic states are represented by:

$$A_1 \quad [|+\rangle|l-\rangle + |-\rangle|l+\rangle]/\sqrt{2}, \quad (5a)$$

$$A_2 \quad [|+\rangle|l-\rangle - |-\rangle|l+\rangle]/\sqrt{2}, \quad (5b)$$

$$E \quad [|+\rangle|l+\rangle \pm |-\rangle|l-\rangle]/\sqrt{2}, \quad (5c)$$

where the double prime for the symmetry species is omitted for simplicity.

First, the Jahn-Teller interaction is considered. This interaction is assumed to be weak, namely to be smaller than the vibrational energy. We also neglect all interactions between the  $\tilde{A}$  state and the other electronic states; namely, we take into account only the matrix el-

ements nonvanishing within the  $\tilde{A}$  state. The first- and second-order Jahn-Teller Hamiltonians are given by

$$\mathbf{H}_{\text{JT}}^{(1)} = V_1 q [e^{i\phi} e^{2i\theta} + e^{-i\phi} e^{-2i\theta}] \quad (6a)$$

and

$$\mathbf{H}_{\text{JT}}^{(2)} = V_2 q^2 [e^{-2i\phi} e^{2i\theta} + e^{2i\phi} e^{-2i\theta}]. \quad (6b)$$

Although the first-order Hamiltonian ( $\mathbf{H}_{\text{JT}}^{(1)}$ ) contributes the same term ( $-k_1^2\omega + k_1^2\omega l\Lambda$ , where  $k_1$  denotes the matrix element of  $V_1$ ,  $\omega$  the vibrational frequency, and  $\Lambda$  a number proportional to the electronic orbital angular momentum component along the symmetry axis) to the two vibronic states ( $A_1$  and  $A_2$ ) under consideration, it is retained because it modifies other terms. In contrast to the first-order Hamiltonian, the second-order Hamiltonian makes different contribution,  $+2k_2\omega$  and  $-2k_2\omega$ , to the  $A_1$  and  $A_2$  states, respectively, lifting the degeneracy of these states, as is well known. It should be noted that the  $E$  state does not receive any terms from the Jahn-Teller interaction, either first-order or second-order; namely, the  $E$  state is separated from the two  $A$  states by the first-order Jahn-Teller term. We thus hereafter neglect this state and focus attention on the two  $A$  states.

We next consider the spin-orbit term, which we assume to be of the form

$$\mathbf{H}_{\text{SO}} = A_{\text{SO}}^{(1)} L_z S_z, \quad (7)$$

i.e. we neglect the perpendicular term  $\frac{1}{2}A_{\text{SO}}^{(2)}(L_+S_- + L_-S_+)$ , because it contains  $L_{\pm}$ . The nonvanishing matrix elements are given by

$$\langle A_1 F_1 | \mathbf{H}_{\text{SO}} | A_2 F_1 \rangle = A_{\text{SO}}^{(1)} \langle L_z \rangle_{\text{eff}} k / \left[ 2 \left( J + \frac{1}{2} \right) \right], \quad (8a)$$

$$\langle A_1 F_2 | \mathbf{H}_{\text{SO}} | A_2 F_2 \rangle = -A_{\text{SO}}^{(1)} \langle L_z \rangle_{\text{eff}} k / \left[ 2 \left( J + \frac{1}{2} \right) \right], \quad (8b)$$

and

$$\begin{aligned} &\langle A_1 F_2 \text{ or } F_1 | \mathbf{H}_{\text{SO}} | A_2 F_1 \text{ or } F_2 \rangle = \\ &-A_{\text{SO}}^{(1)} \langle L_z \rangle_{\text{eff}} \left[ \left( J + \frac{1}{2} \right)^2 - k^2 \right]^{\frac{1}{2}} / \left[ 2 \left( J + \frac{1}{2} \right) \right], \quad (8c) \end{aligned}$$

where the matrix element of the electron orbital angular momentum is equal to

$$\langle L_z \rangle_{\text{eff}} = \zeta_e (1 - 4k_1^2). \quad (9)$$

In Eqs. 8a, 8b, and 8c,  $F_1$  and  $F_2$  denote the two spin components:  $J = N + \frac{1}{2}$  and  $J = N - \frac{1}{2}$  for  $F_1$  and  $F_2$ , respectively (in the present case, the electron spin quantum number  $S = 1/2$ ). The electronic Coriolis coupling constant is designated as  $\zeta_e$  in Eq. 9.

The next term that we should consider is the electronic and vibrational Coriolis term, of which we retain only the  $z$  term, i.e. the term associated with the symmetry axis. The matrix elements are nonvanishing only between the  $A_1$  and  $A_2$  blocks of the same spin sublevels:



$$\begin{aligned} \langle A_1 F_1 | \mathbf{H}_{\text{Cor}} | A_2 F_1 \rangle &= \langle A_1 F_2 | \mathbf{H}_{\text{Cor}} | A_2 F_2 \rangle \\ &= -2C \langle L_z \rangle_{\text{eff}} k + 2C \langle \pi_z \rangle_{\text{eff}} k, \quad (10) \end{aligned}$$

where the vibrational angular momentum matrix element means

$$\langle \pi_z \rangle_{\text{eff}} = \zeta_{v,z} (1 + 2k_1^2), \quad (11)$$

with  $\zeta_{v,z}$  denoting the vibrational Coriolis coupling constant.

We employ the ordinary expressions for the spin-rotation interaction and the pure rotation terms, and the matrix elements of them are given by:

$$\langle F_1 | \mathbf{H}_{\text{SR}} | F_1 \rangle = E_{\text{SR}} - (\epsilon_{bb}/2), \quad (12a)$$

$$\langle F_2 | \mathbf{H}_{\text{SR}} | F_2 \rangle = -E_{\text{SR}} - (\epsilon_{bb}/2), \quad (12b)$$

and

$$\begin{aligned} \langle F_2 | \mathbf{H}_{\text{SR}} | F_1 \rangle &= \\ &= -(\epsilon_{cc} - \epsilon_{bb})k \left[ \left( J + \frac{1}{2} \right)^2 - k^2 \right]^{\frac{1}{2}} / \left[ 2 \left( J + \frac{1}{2} \right) \right], \quad (12c) \end{aligned}$$

where

$$E_{\text{SR}} = (\epsilon_{cc} - \epsilon_{bb})k^2 / \left[ 2 \left( J + \frac{1}{2} \right) \right] + (\epsilon_{bb}/2) \left( J + \frac{1}{2} \right) \quad (12d)$$

and

$$\langle F_1 | \mathbf{H}_{\text{R}} | F_1 \rangle = E_{\text{R}}(1) + E_{\text{R}}(2), \quad (13a)$$

$$\langle F_2 | \mathbf{H}_{\text{R}} | F_2 \rangle = E_{\text{R}}(1) - E_{\text{R}}(2), \quad (13b)$$

where

$$\begin{aligned} E_{\text{R}}(1) &= (B - D_N) \left( J + \frac{1}{2} \right)^2 + (C - B)k^2 \\ &\quad - D_N \left( J + \frac{1}{2} \right)^4 - D_{NK} \left( J + \frac{1}{2} \right)^2 k^2 - D_K k^4, \quad (13c) \end{aligned}$$

$$E_{\text{R}}(2) = -B \left( J + \frac{1}{2} \right) + 2D_N \left( J + \frac{1}{2} \right)^3 + D_{NK} \left( J + \frac{1}{2} \right) k^2. \quad (13d)$$

The molecular parameters appearing in Eqs. 10, 11, 12, and 13 are assumed to be the same for the two A states. The energy matrix for the four levels, the  $F_1$  and  $F_2$  spin levels of both the  $A_1$  and  $A_2$  states, is thus given by

$$\begin{vmatrix} 2k_2\omega + [\delta] & [\epsilon] & [\alpha] & [\beta] \\ [\epsilon] & 2k_2\omega - [\delta] & [\beta] & -[\alpha] \\ [\alpha] & [\beta] & -2k_2\omega + [\delta] & [\epsilon] \\ [\beta] & -[\alpha] & [\epsilon] & -2k_2\omega - [\delta] \end{vmatrix}, \quad (14a)$$

where

$$\begin{aligned} [\delta] &= E_{\text{R}}(2) + E_{\text{SR}} \\ &= -B \left( J + \frac{1}{2} \right) + 2D_N \left( J + \frac{1}{2} \right)^3 + D_{NK} \left( J + \frac{1}{2} \right) k^2 \\ &\quad + (\epsilon_{cc} - \epsilon_{bb})k^2 / \left[ 2 \left( J + \frac{1}{2} \right) \right] + (\epsilon_{bb}/2) \left( J + \frac{1}{2} \right), \quad (14b) \end{aligned}$$

$$[\epsilon] = -(\epsilon_{cc} - \epsilon_{bb})k \left[ \left( J + \frac{1}{2} \right)^2 - k^2 \right]^{\frac{1}{2}} / \left[ 2 \left( J + \frac{1}{2} \right) \right], \quad (14c)$$

$$[\alpha] = A_{\text{SO}}^{(1)} \langle L_z \rangle_{\text{eff}} k / \left[ 2 \left( J + \frac{1}{2} \right) \right] - 2C [\langle L_z \rangle_{\text{eff}} - \langle \pi_z \rangle_{\text{eff}}] k, \quad (14d)$$

and

$$[\beta] = A_{\text{SO}}^{(1)} \langle L_z \rangle_{\text{eff}} \left[ \left( J + \frac{1}{2} \right)^2 - k^2 \right]^{\frac{1}{2}} / \left[ 2 \left( J + \frac{1}{2} \right) \right]. \quad (14e)$$

The terms common to the four blocks,  $-2k_1^2\omega + E_{\text{R}}(1) - \epsilon_{bb}/2$ , have been subtracted from each of the diagonal elements of the matrix. The matrix is readily solved to give the following eigenvalues:

$$\begin{aligned} E &= (B - D_N) \left( J + \frac{1}{2} \right)^2 + (C - B)k^2 - D_N \left( J + \frac{1}{2} \right)^4 - D_{NK} \left( J + \frac{1}{2} \right)^2 k^2 \\ &\quad - D_K k^4 \pm \{ 4k_2^2\omega^2 + [\delta]^2 + [\epsilon]^2 + [\alpha]^2 + [\beta]^2 \\ &\quad \pm 2[(\alpha)[\delta] + [\beta][\epsilon]]^2 + 4k_2\omega^2([\delta]^2 + [\epsilon]^2) \}^{\frac{1}{2}}, \quad (15) \end{aligned}$$

where the plus sign of the first double sign applies to the levels of the  $A_1$  state, provided that  $k_2$  is positive.

### Silicon Hydrides

Much interest has been paid to silicon compounds, particularly in comparing their chemistry with that of the corresponding carbon analogues; silicon hydrides serve as typical examples in this respect. It has also been recognized that the hydrides play important roles in a silane discharge plasma, which has been extensively employed in the processing of electronic devices. In the discharge of silane several intermediate species must be present; some of them play key roles in the chemical and physical processes taking place in the plasma. It is, therefore, of great significance to identify any intermediate chemical species in the plasma, to unveil their dynamical behaviors, and to determine their population distributions over the quantum states in real time. To accomplish such objectives, we need to know the spectra, preferably of high resolution, of the important intermediates. Yamada and Hirota<sup>62)</sup> have thus initiated a study of the  $\nu_2$  band of the silyl radical by using an infrared diode-laser spectrometer.

In contrast with the methyl radical, which has been confirmed to be planar in the ground electronic state,<sup>63)</sup> although the silyl radical was predicted to be nonplanar, the barrier height at the planar configuration was estimated to be so low that the molecule could invert quite easily, like ammonia.<sup>64)</sup> Yamada and Hirota, in fact, found that the  $\nu_2$  band appeared to be split into two components ( $1^- \leftarrow 0^+$  and  $1^+ \leftarrow 0^-$ ) at 727.9438 (11) and 721.0486 (9)  $\text{cm}^{-1}$ , respectively, where the + and - superscripts denoted the symmetric and antisymmetric inversion levels, respectively. Johnson et al.<sup>65)</sup> have subsequently recorded the multiphoton ionization spectra of  $\text{SiH}_3$  and  $\text{SiD}_3$ , and detected two Rydberg states. They also determined the ionization potential and the energy levels of  $\nu_2''$  up to 3 and 4 for  $\text{SiH}_3$  and  $\text{SiD}_3$ , respectively, in the ground electronic state, from which they calculated the inversion potential to be 1935 and 1925



$\text{cm}^{-1}$  for the two isotopic species. Yamada and Hirota have estimated the inversion splitting to be 0.144 and  $6.75 \text{ cm}^{-1}$  in the  $\nu_2=0$  and 1 states, respectively. They also derived the structure parameters:  $r(\text{Si-H})=1.468 \text{ \AA}$  and  $\theta(\text{H-Si-H})=110.5^\circ$ .

The  $\nu_2$  vibration-rotation spectral lines of  $\text{SiH}_3$  thus observed have been employed by Itabashi et al.<sup>66-69)</sup> to diagnose the silane discharge plasma. Although it had been suspected that  $\text{SiH}_3$  played key roles in the plasma, unfortunately, no reliable methods had been available before to determine the population distribution of this important species. Itabashi et al. have determined the density, diffusion coefficient, reaction rates, and spatial distribution of silyl in both rf and pulsed-discharge plasmas of silane, and have concluded that  $\text{SiH}_3$  is by far the most abundant species and dominates the process of the formation of amorphous silicon film on a substrate.

Recently, Sumiyoshi et al.<sup>70)</sup> have detected  $\nu_3$ , i.e. the Si-H degenerate stretching band, of  $\text{SiH}_3$  in  $5 \mu\text{m}$  region. This band will be stronger than the  $\nu_2$  band by a factor of 3 or so, and, thus, is much more useful for monitoring the silyl radical. However, the  $\nu_3$  band is in Coriolis resonance with  $\nu_1$ , i.e. the Si-H symmetric stretching band; this interaction must be fully analyzed before the  $\nu_3$  band can be employed for a quantitative analysis.

The second silicon hydride  $\text{SiH}_2$  is a species known in molecular spectroscopy for a long time; it was in 1967 that Dubois et al.<sup>71)</sup> observed the absorption spectrum of  $\text{SiH}_2$  in the visible region for the first time. Dubois<sup>72)</sup> and Dubois et al.<sup>73)</sup> subsequently analyzed the rotational structures of the  $\tilde{\text{A}}^1\text{B}_1 \leftarrow \tilde{\text{X}}^1\text{A}_1$  ( $0\nu_2^0$ )—(000) bands with  $\nu_2'=1-3$  and  $4-6$ , respectively. This  $\tilde{\text{A}}-\tilde{\text{X}}$  band has recently been reinvestigated in more detail by Ishikawa and Kajimoto<sup>74,75)</sup> as well as by Fukushima et al.<sup>76,77)</sup>

Yamada et al.<sup>78)</sup> have applied infrared diode-laser spectroscopy to the  $\nu_2$  band of  $\text{SiH}_2$  in the ground electronic state in order to obtain more precise information concerning this molecule. The band origin that they determined is  $998.6241 (3) \text{ cm}^{-1}$ , which may be compared with the  $1004 \text{ cm}^{-1}$  that Dubois<sup>72)</sup> obtained from a hot band of the electronic transition in the visible region. Yamada et al. calculated the so-called  $r_0$  structure parameters [ $r_0(\text{Si-H})=1.525 (6) \text{ \AA}$  and  $\theta_0(\text{H-Si-H})=91.8 (10)^\circ$ ] from the observed rotational constants. They also utilized a similarity in the structure of  $\text{SH}_2$  and  $\text{SiH}_2$  to estimate the equilibrium structure:  $r_e(\text{Si-H})=1.5140 \text{ \AA}$  and  $\theta_e(\text{H-Si-H})=92.08^\circ$ . The observed centrifugal distortion constants and inertial defect were used to calculate the harmonic force constants, which were then combined with the vibration-rotation constants ( $\alpha_2$ ) to derive two cubic anharmonic potential constants:  $k_{222}=-15.75$  and  $k_{122}=53.01$  in  $\text{cm}^{-1}$ . The latter  $k$  constant should be useful in analyzing the Fermi interaction between  $\nu_1$  and  $2\nu_2$ .

The thus-observed  $\nu_2$  band was unfortunately found

to be quite weak, and it has been used only for a qualitative or semiquantitative analysis. Yamada et al.<sup>79)</sup> have thus extended measurements to the spectra in the  $5 \mu\text{m}$  region, where we expect to observe three vibrational bands ( $\nu_1$ ,  $2\nu_2$ , and  $\nu_3$ ). The three excited states of these bands interact with each other by Fermi (between  $\nu_1$  and  $2\nu_2$ ) and Coriolis (between  $\nu_1$  and  $\nu_3$  and also between  $2\nu_2$  and  $\nu_3$ ) resonance. In addition, the three band origins are expected to be quite close to each other. In fact, the observed spectral lines do not show any spectral patterns which readily lead to assignments.

One problem remaining to be solved for this molecule is detecting the lowest triplet. As is well known, the carbon analogue of this molecule, carbene  $\text{CH}_2$ , has a triplet ground state  $\tilde{\text{X}}^3\text{B}_1$ , and the lowest excited state ( $\tilde{\text{a}}^1\text{A}_1$ ) lies at  $3165 \pm 20 \text{ cm}^{-1}$  [ $\text{T}_{00}$ ] above the ground state.<sup>80)</sup> In contrast, the ground electronic state of  $\text{SiH}_2$ , i.e. silylene, is singlet  $\tilde{\text{X}}^1\text{A}_1$ , and the lowest excited state is a triplet, which has been predicted to lie at about  $7345 \pm 350 \text{ cm}^{-1}$  above the ground state,<sup>81)</sup> but has not been detected experimentally.

The third hydride  $\text{SiH}$  is a typical  $^2\Pi_r$  molecule in the ground electronic state, and has already been extensively investigated by high-resolution spectroscopy in the ultraviolet, visible, and infrared regions.

Investigations of a silane discharge plasma require information concerning any intermediate species which contain more than one silicon atom. However, spectroscopic data on those molecules have been very rare. Among molecules with two silicon atoms, only two species have been subjected to spectroscopic studies:  $\text{Si}_2\text{H}_6$  and  $\text{Si}_2\text{H}_2$ . The latter molecule, disilyne ( $\text{Si}_2\text{H}_2$ ), is very interesting; it exists in two forms, both of which are completely different in geometry from acetylene: one [ $\text{Si}(\text{H})_2\text{Si}$ ] with two silicon atoms doubly bridged by hydrogens and of  $C_{2v}$  symmetry<sup>82,83)</sup> and the other [ $\text{Si}(\text{H})\text{SiH}$ ] monobridged leaving the other hydrogen attached in the molecular plane to one of the two silicon atoms.<sup>84)</sup> Other molecules with two Si atoms, such as  $\text{Si}_2\text{H}_4$ , must wait for further spectroscopic studies.

High-resolution spectroscopic data are also available for a few cations of monosilicon hydrides. The simplest one,  $\text{SiH}^+$ , is a diatomic molecule; its electronic spectrum has been quite well known. Recently, Davies and Martineau<sup>85)</sup> have reported on its fundamental band in the infrared.

The  $\text{SiH}_2^+$  ion has been a subject of electronic spectroscopy where special attention was paid to predissociation in the excited electronic states. However, neither the vibrational nor rotational spectra have been reported.

The third monosilicon hydride ion,  $\text{SiH}_3^+$ , was recently investigated by Davies et al.<sup>86,87)</sup> using infrared diode-laser spectroscopy. Davies and Smith have observed and analyzed the  $\nu_2$  and  $\nu_4$  bands simultaneously, because the two upper vibrational states are coupled by a Coriolis interaction. It may be worth noting

that  $\text{SiH}_3^+$  is a planar molecule, as expected from a Walsh diagram.

### Projects in Future

In concluding the present article, a few projects are listed for which some preliminary studies have already been carried out, but discontinued for some reasons, or are still continuing. These projects are certainly worth being pursued further and being completed in the near future.

**Internal Motions of Ions in Inorganic Molecules: Alkali Tetrahydroborates.** Most inorganic compounds are solid at room temperature. It is thus not easy to foresee whether they also exist in forms of molecules in the gaseous phase. For example, since ammonium chloride has been known to sublime quite easily, this characteristic has been employed for purification. One might then ask the question as to whether it exists in a form of  $\text{NH}_4\text{Cl}$  or dissociates into  $\text{NH}_3$  and  $\text{HCl}$ , or forms aggregates or clusters during sublimation. A clear answer was given only quite recently; Goodwin et al.<sup>88)</sup> and Howard and Legon<sup>89)</sup> have shown that a major component of gaseous ammonium chloride is a  $C_{3v}$  symmetric top with the nuclei in the order  $\text{H}_3\text{NHCl}$ , i.e. a hydrogen-bonded complex. However, because the method employed in these studies prepared molecules at very low temperature, there still remains a possibility that other forms might also exist when ammonium chloride is sublimed at much higher temperature. In any case, it is quite interesting to make inorganic substances gaseous molecules, because they often take unexpected configurations in the gaseous phase.

The ionic bonds are quite common in inorganic molecules. The ions often consist of a group of atoms, as exemplified by  $\text{NH}_4^+$ ,  $\text{NO}_3^-$ , and  $\text{CO}_3^-$ . These ions may execute internal motions as a whole which are not common in organic molecules. Kawashima and his collaborators<sup>90–92)</sup> have recently carried out a systematic study on vaporized alkali tetrahydroborates,  $\text{MBH}_4$  ( $\text{M}=\text{Li}, \text{Na}, \text{and K}$ ), by using microwave spectroscopy. They have shown that these molecules consist of an alkali cation and a tetrahydroborate anion:  $\text{M}^+ \text{BH}_4^-$  and that  $\text{M}^+$  is bonded to  $\text{BH}_4^-$  through three hydrogens, namely the molecule takes a tridentate configuration at the equilibrium. The microwave spectrum of these molecules in the ground vibrational states fits nicely to a pattern expected for a  $C_{3v}$  symmetric top. The ground-state rotational spectrum is accompanied by two sets of vibrational satellites; one is assigned to the first excited state of the  $\text{M}^+-\text{BH}_4^-$  stretching vibration, which belongs to  $A_1$  symmetry, and the other to that of the  $\text{BH}_4$  degenerate rocking vibration, which is of E symmetry. The two sets of satellites are interacting with each other by Coriolis resonance, and the perturbation is most extensive in the case of Na, in which the two vibrational states differ in energy by only  $24 \text{ cm}^{-1}$ , and also to a considerable extent for the

K derivative where the two modes are separated by  $48 \text{ cm}^{-1}$ . These interactions obscure the effects on the rotational spectra caused by the motion of the  $\text{BH}_4^-$  ion. In contrast, the Li molecule gives clean satellite spectra; Kawashima and Hirota have analyzed the observed spectra, each satellite separately, in detail.

Kawashima and Hirota<sup>91)</sup> have noticed two anomalies for the satellite of the  $\text{BH}_4$  rocking vibration of  $\text{LiBH}_4$ . One applies to the so-called 2, -1 interaction constant (designated as  $r_t$ ), which is determined to be  $388.23 (14) \text{ MHz}$ , much larger in magnitude than the 2,2 interaction constant ( $q_t$ ) of  $-137.578 (56) \text{ MHz}$ ; the suffix ( $t$ ) denotes the degenerate  $\text{BH}_4$  rocking vibration. The second anomaly is a slight, but definite, increase in the  $D_{JK}$  centrifugal distortion constant when the  $\text{BH}_4$  rocking mode is excited; its value [ $1.1214 (11) \text{ MHz}$ ] is compared with the ground-state value [ $0.8268 (17) \text{ MHz}$ ] or with that in the Li- $\text{BH}_4$  stretching excited state [ $0.7997 (19) \text{ MHz}$ ]. Such a large change is not observed for  $D_J$  [ $0.10316 (18)$ ,  $0.10810 (20)$ , and  $0.10413 (12) \text{ MHz}$  for the ground, stretching, and rocking states, respectively].

Hirota and Kawashima<sup>93)</sup> have explained these two anomalies in the following way. They first noticed that the  $xz$  and  $yz$  cross products of the inertia strongly depend on the  $\text{BH}_4$  rocking coordinate; in other words, the first order coefficients ( $a_t^{(xz)}$  and  $a_t^{(yz)}$ ) in the expansion of the moments of inertia in terms of the rocking coordinate are anomalously large. Here,  $z$  denotes the symmetry axis and  $x$  and  $y$  stand for the two perpendicular inertial axes. This coefficient, together with a cubic anharmonic potential constant ( $k_{ttt}$ ) makes the following contribution to the  $r_t$  constant:

$$2\pi AB \left[ 3a_t^{(xz)} / (h\nu_t^3)^{\frac{1}{2}} \right] k_{ttt}. \quad (16)$$

Although there is a corresponding term for  $q_t$ ,  $a_t^{(xz)}$  is replaced by  $a_t^{(xx)}$  there, which is almost zero; the so-called harmonic term dominates in  $q_t$ . The change in the  $D_{JK}$  constant with excitation of the  $\text{BH}_4$  rocking vibration is also ascribed primarily to  $a_t^{(xz)}$  combined with anharmonic potential constants associated with the  $\text{BH}_4$  rocking vibration. It should be noted that the centrifugal distortion constants, themselves, are derived by second-order perturbation of vibration-rotation interactions, and do not depend on the vibrational quantum numbers explicitly; in other words, they remain the same in all of the vibrational states. The changes in the centrifugal distortion constants with vibrations are introduced by higher-order perturbations, but are normally quite small. In the present case, the change in  $D_{JK}$ , or more exactly, in  $D_{JK} + 2D_J$ , is obtained by third-order perturbation involving a quartic anharmonic potential constant ( $f_{tttt}$ ) and also by fourth-order perturbation with ( $k_{ttt}$ ):

$$\Delta(D_{JK} + 2D_J)_t = 32\pi^2 A^2 B^2 \left[ (a_t^{(xz)})^2 / (h\nu_t^2) \right] \times [-8(f_{tttt}/\nu_t) + 9(k_{ttt}/\nu_t)^2]. \quad (17)$$

The two anomalies are explained by inserting the following values in the two anharmonic potential constants:

$$k_{ttt} = -34.89 \text{ and } f_{ttt} = -10.84 \text{ cm}^{-1}.$$

The interaction potential between the  $\text{Li}^+$  and  $\text{BH}_4^-$  ions may be approximated by a multipole expansion, although the distance between the two ions is not much larger than the radius of  $\text{BH}_4^-$ , making the convergence of the expansion rather slow. Although the lowest order term in the expansion consists of an octupole moment ( $Q_3$ ), this single term is not sufficient to reproduce the potential function calculated by an *ab initio* molecular orbital (MO) method; the ratio of two potential barrier heights, one at a monodentate and the other at bidentate configuration ( $V_M/V_B$ ) equals to 2 in the multipole expansion, which is to be compared with the MO ratio (4.1) calculated by Uemura.<sup>94</sup> The next lowest order term in  $Q_4$  is therefore included so as to reproduce the *ab initio* MO ratio of  $V_M/V_B$ . It should be noted that the next term in  $Q_5$  in the multipole expansion is zero because of symmetry. We thus have the following expressions for the harmonic force constant ( $f_t$ ) and two anharmonic potential constants ( $k_{ttt}$  and  $f_{ttt}$ ):

$$f_t = -(40/3)Q_3(1 + 7Q_4/9Q_3), \quad (18a)$$

$$k_{ttt} = (10\sqrt{2}Q_3/9)(1 - 7Q_4/3Q_3)(2F/\nu_t)^{3/2}, \quad (18b)$$

and

$$f_{ttt} = (85Q_3/18)(1 + 203Q_4/153Q_3)(2F/\nu_t)^2, \quad (18c)$$

where  $F$  denotes the "rotational" constant for the  $\text{BH}_4$  group internal rotation. The  $Q_3$  constant is chosen so as to reproduce the harmonic frequency of the  $\text{BH}_4$  rocking vibration of  $400 \text{ cm}^{-1}$ , whereas the ratio ( $Q_4/Q_3$ ) is fixed to a value that is consistent with the *ab initio*  $V_M/V_B$  ratio. Then,  $k_{ttt}$  and  $f_{ttt}$  are calculated to be  $-23.1$  and  $-2.24 \text{ cm}^{-1}$ , respectively, which are in qualitative agreement with the observed values,  $-34.89$  and  $-10.84 \text{ cm}^{-1}$ .

When the amplitude of the  $\text{BH}_4^-$  rocking vibration becomes large, the  $\text{BH}_4$  group may overpass one of the saddle points in the potential surface, possibly one of the bidentate configurations, to enter into a neighboring tridentate minimum. Hirota<sup>95</sup> has discussed the effects of internal motion of the  $\text{BH}_4$  group on the rotational spectrum. There are four equivalent minima, i.e. tridentate configurations, which are grouped in A and F species in a  $T$  point group. A high barrier approximation, i.e. an approach in which the internal rotation of  $\text{BH}_4$  is assumed to be much larger in energy than the overall rotation, will be appropriate in the present case. This approximation looks similar to PAM (principal axis method) in the treatment of the internal rotation of a methyl group. Hirota derived second-order corrections for the  $B$  rotational constant as

$$\text{A block: } (4B^2/F)w \text{ and F block: } -(4B^2/3F)w, \quad (19)$$

where  $w$  denotes a second-order sum given by

$$w = \sum_{v'} |\langle v | j | v' \rangle|^2 / \Delta E_{v,v'}, \quad (20)$$

with  $j$  denoting the angular momentum of the  $\text{BH}_4$  group internal rotation,  $v$  and  $v'$  two internal rotation states, and  $FE_v$  the eigenvalue of the internal rotation. For the F block there are additional  $\Delta k = \pm 2$  terms; also,  $\Delta k = \pm 1$  terms contribute to both of the A and F states. However, these additional terms will be less important than those given in Eq. 19. Kawashima and Hirota<sup>96</sup> have observed rotational lines of  $\text{LiBH}_4$  which are possibly ascribed to the  $v_t = 2$  state, but have not assigned them.

**Transient Molecules of Astronomical Interest: the  $\text{C}_3\text{H}_3^+$  Ion.** The number of interstellar molecules so far detected by radiotelescopes approaches one hundred. It is remarkable that about half of them are transient molecules and their fractions seem to be even increasing. In view of the low temperature and low density of the environment in interstellar space, this trend may not be surprising, and encourages further spectroscopic detection of many more short-lived species in the laboratory which can be of some astronomical significance.

Besides identification of new molecular species with short lifetimes, we should also pay attention to metastable states; molecules in these states have been referred to as *isomers* in chemistry. In low-temperature interstellar space, even low potential barriers between isomers are often sufficient to stabilize molecules in metastable states and to isolate them from those in the ground state, even in cases where such trapping is difficult to perform under laboratory conditions. The most well-known example of an isomer found in interstellar space is HNC, which, although higher in energy by about  $0.447 (48) \text{ eV}$ ,<sup>97</sup> is as abundant as the parent molecule (HCN) in dark molecular clouds, supporting an important hypothesis that both of the species are formed primarily by a dissociative recombination of  $\text{HCNH}^+$  with an electron. Recently, Kawaguchi et al. succeeded in detecting two isomers of cyanoacetylene HCCCN in TMC-1 ( $\text{HCCNC}$ <sup>98</sup>) and  $\text{HNCCC}$ <sup>99</sup>) which are about 60 and 450 times less abundant than their parent molecule (HCCCN), respectively. More recently, Kawaguchi and his collaborators<sup>100</sup> detected a protonated ion ( $\text{HCCCNH}^+$ ), again in TMC-1, which was long-standing in a list of molecules to be detected in interstellar space; its abundance was about  $1/160$  of HCCCN. Granted that  $\text{HCCNC}$  and  $\text{HNCCC}$  are less stable than HCCCN by  $0.8$  and  $2.2 \text{ eV}$ ,<sup>101</sup> the observations of Kawaguchi et al. are rather difficult to reconcile with a naive dissociative recombination model widely accepted and seem to suggest that there are other important chemical routes to end up in the two isomers of HCCCN. This study clearly indicates that isomers, or better expressed, metastable species, bring about infor-

mation of considerable significance, not only for molecular-structure studies, but also for astronomical investigations.

Another important direction in molecular astronomy would be the detection of nonpolar transient molecules, both in laboratory and interstellar space. Because most nonpolar molecules do not give pure rotational spectra, we must have recourse to other methods. Among them, infrared spectroscopy would be the most promising. Only a little over ten molecules have so far been detected in space by infrared telescopes; among them, CN, CCH, CCC, and CCCCC are transient molecules. There are certainly many more species that play far more important roles in interstellar chemistry. We may mention  $\text{H}_3^+$ ,  $\text{CH}_3$ ,  $\text{CH}_3^+$ , and  $\text{C}_3\text{H}_3^+$ . The last cation, which presumably belongs to the high symmetry of  $D_{3h}$ , has been reported by using mass spectrometry to be quite abundant in systems consisting of carbon and hydrogen, such as discharge plasma in hydrocarbons. Yamada<sup>102)</sup> examined a region around  $1300\text{ cm}^{-1}$  on a discharge system involving a mixture of acetylene and oxygen by using an infrared diode laser spectrometer; although he observed a few lines, he could not confirm whether those lines were ascribed to  $\text{C}_3\text{H}_3^+$ . Two *ab initio* calculations<sup>103,104)</sup> have recently been performed on the ion; the calculated vibrational frequencies are compared with those of the ion which exists together with a counterion in condensed phases.<sup>105)</sup>

**Development of High-Resolution Kinetic Spectroscopy and Its Applications to the Mechanisms of Chemical Reactions: Ally-Cyclopropyl Interconversion Reaction and Ring Contraction Reaction of Dodecamethylcyclohexasilane.**

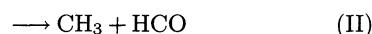
Subpicosecond and femtosecond spectroscopy have been becoming routine in the field of reaction dynamics. However, a number of interesting problems still remain in the field which do not necessarily require the highest speed of the laser technology presently available, but may be nicely solved by high resolution rather than by the high speed of spectroscopic methods. Kanamori et al.<sup>106)</sup> and Endo et al.<sup>107)</sup> have developed infrared and microwave kinetic spectroscopies using infrared diode lasers and millimeter-wave klystrons as sources, and have applied them to a few chemical reactions so as to unveil their mechanisms in detail. Suzuki et al.,<sup>108)</sup> for example, examined the photolysis of methyl iodide at 248 nm by a time-resolved observation of the methyl radical  $\nu_2$  bands. This famous reaction had been investigated by several groups before, but, because most of them employed mass spectrometry, they could not have obtained the population distributions of methyl on individual vibration-rotation quantum state. Nevertheless, these previous investigators claimed that they obtained the vibrational distribution of methyl peaking at the  $\nu_2=2$  level; some theoreticians rationalized these results by "adjusting" their calculations. Although Suzuki et al. employed an ordinary sample cell, not a molecular-

beam nozzle, they have derived the vibrational distribution of methyl without being affected by intermolecular collisions. They thus clearly showed that the nascent distribution of methyl radicals monotonously decreased with the  $\nu_2$  quantum number. It is rather difficult to understand why so many groups arrived at the same erroneous conclusion; the main reason would be the lack of spectral resolution of the methods employed.

Another example is the oxidation reaction of ethylene. Most people had agreed that this reaction had two main channels:



and

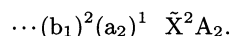


and that reaction (II) took place only at pressures larger than several hundred Torr (several ten kPa), i.e. (II) was a pressure-induced reaction. It should be noted that the second conclusion was derived based upon a molecular-beam study,<sup>109)</sup> which did not detect the two products expected for reaction (II); namely, the second conclusion merely represented a hypothesis to justify the conclusion of the molecular-beam experiment. Endo et al.<sup>110)</sup> examined this reaction using microwave kinetic spectroscopy; in this experiment the sample pressure was about 0.03 Torr (4 Pa), well in the low-pressure region. Contrary to the second conclusion, Endo et al. arrived at a branching ratio 0.4:0.5 for (I):(II), which was essentially identical to that obtained under the high-pressure condition. Again, the discrepancy was caused by an improper use of mass spectrometry in the molecular-beam experiment, which was later revised by repeating the detection of the reaction products more carefully with isotopic samples.<sup>111)</sup> The new measurement agreed with the microwave result of Endo, and the hypothesis was thrown away.

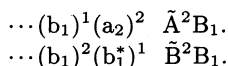
There are a number of chemical reactions remaining to which high-resolution kinetic spectroscopy, either infrared or microwave, may be successfully applied. Here, two possible cases are mentioned:

**(1) The Ring-Closing and Ring-Opening Reactions between the Allyl and Cyclopropyl Radicals.**

The lowest-lying electronic states of allyl may be given in terms of three  $\pi$  orbitals, one on each of the three carbon atoms. Because allyl belongs to  $C_{2v}$  symmetry,<sup>112)</sup> we may combine the three  $\pi$  orbitals such that we have two orbitals of  $b_1$  and one orbital of  $a_2$  symmetry; one of the two  $b_1$  orbitals is bonding and the other antibonding (designated hereafter as  $b_1^*$ ), whereas the  $a_2$  orbital is essentially nonbonding. The ground electronic state is thus represented by the following electronic configuration:



We may generate two low-lying excited electronic states as follows:



Currie and Ramsay<sup>113)</sup> reported on an observation of the  $\tilde{A}$ - $\tilde{X}$  system, the 0-0 band of which appeared at 408.3 nm. The first observation of the  $\tilde{B}$ - $\tilde{X}$  transition was made by Callear and Lee,<sup>114)</sup> who observed a strong, but diffuse, system in the 210–250 nm region.

The ring-closing reaction from allyl to cyclopropyl may proceed along either one of two possible pathways, namely with two methylene groups rotating in an opposite way (referred to as *disrotatory*) or in a similar way (as *conrotatory*) when viewed from the central carbon atom. In the *disrotatory* case, the molecule will keep  $C_s$  symmetry; we label each molecular orbital as either  $a'$  or  $a''$ . The  $b_1$  and  $b_1^*$  orbitals of allyl thus become  $7a'$  and  $8a'$ , while the  $a_2$  orbital is renamed as  $5a''$ . The corresponding orbitals of cyclopropyl are  $7a'$ ,  $8a'$ , and  $5a''$  in increasing order of energy. Therefore, the top two orbitals must cross somewhere between allyl and cyclopropyl. As a result, we can see that the ground state of allyl does *not* go over to the ground state of the cyclopropyl, but to an excited state of the latter, and vice versa.

In the case of a *conrotatory* path, although the molecule maintains  $C_2$  symmetry near to the allyl configuration, the symmetry gradually changes to  $C_s$  as the molecule approaches the cyclopropyl configuration. It is somewhat difficult to classify the energy levels according to their symmetry; however, because  $C_2$  symmetry is only slightly broken by the out-of-plane bending of the  $\alpha$  C-H bond of cyclopropyl, we assume that the  $C_2$  symmetry is maintained during the process. We thus label the molecular orbitals either  $a$  or  $b$ . The allyl orbitals then become  $5b$ ,  $7a$ , and  $6b$ , while those of cyclopropyl are  $7a$ ,  $5b$ , and  $6b$ . Hence, crossing in this case takes place between the two lowest orbitals. The ground states of the two molecules again do not correlate with each other, but with an excited electronic state. These interesting properties of the allyl-cyclopropyl conversion were pointed out by Longuet-Higgins and Abrahamson<sup>115)</sup> for the first time in 1965.<sup>116)</sup>

It would be interesting to quote a resonance Raman study of Getty et al.,<sup>117)</sup> who employed the  $\tilde{B}$  state as an intermediate state and observed six vibrational bands of allyl in the ground electronic state. They noticed that the vibrational coordinates of all of these six bands corresponded well to the geometry changes expected when allyl was converted to cyclopropyl. This statement can be well understood based on the correlation diagram for the *disrotatory* case; allyl excited to the  $\tilde{B}$  state smoothly moves to the ground state of cyclopropyl.

In contrast with allyl, few spectroscopic data have been published on cyclopropyl. Holtzhauer et al.<sup>118)</sup> generated cyclopropyl by converting allyl trapped in a low-temperature argon matrix with the irradiation of 410 nm light. This photoconversion corresponds to an exci-

tation of allyl to the  $\tilde{A}$  state; thus, the path would be *conrotatory*. Holtzhauer et al. reported on the infrared absorption spectrum of cyclopropyl thus obtained; however, the intensities of the individual bands do not match well with the values predicted by Olivella,<sup>119)</sup> suggesting that the matrix IR spectra of Holtzhauer need to be refined.

According to Olivella's calculation, the three bands ( $\nu_8$ ,  $\nu_{10}$ , and  $\nu_{17}$ ) predicted to appear at 830, 630, and 900  $\text{cm}^{-1}$ , respectively, would be best observed by infrared diode-laser spectroscopy. Okunishi and Hirota<sup>120)</sup> have thus tested the excimer-laser photolysis at 193 or 248 nm of several precursors, including cyclopropyl bromide and dicyclopropyl ketone, but could not observe any absorptions. K. U. Ingold<sup>121)</sup> has suggested either cyclopropyl iodide or the *t*-butyl ester of cyclopropaneperoxycarboxylic acid [ $c\text{-C}_3\text{H}_5\text{C}(\text{O})\text{OOC}(\text{CH}_3)_3$ ] as being the best precursor. Another possible way to generate cyclopropyl would be a route through the  $\tilde{B}$  state, rather than the  $\tilde{A}$  state of allyl, as done in Holtzhauer's experiment; the  $\tilde{B}$ - $\tilde{X}$  transition is stronger than the  $\tilde{A}$ - $\tilde{X}$  transition, and, furthermore, the 248 nm line of a  $\text{Kr}^+$  laser is close to the  $\tilde{B}$ - $\tilde{X}$  band origin.<sup>122)</sup>

The direct process between the ground states of the two molecules are also interesting. Although it is forbidden as long as the two  $\text{CH}_2$  groups are equivalent, it can be induced by making two  $\text{CH}_2$  inequivalent. For example, we may excite cyclopropyl to a vibrational state of  $a''$  symmetry;  $\nu_{17}$  or  $\nu_{12}$  would be a good candidate.

**(2) Ring Contraction Reactions of Some Cyclic Silicon Compounds; Detection of an Intermediate Species Dimethylsilylene.** Organosilicon compounds exhibit many interesting chemical properties. One fascinating example is the ring contraction of dodecamethylcyclohexasilane, which was investigated by Ishikawa and Kumada<sup>123)</sup> for the first time. They found that, when the precursor compound was irradiated at 254 nm, the ring contraction took place along with a cleavage of dimethylsilylene. The same reaction was repeated by Drahnak et al.<sup>124)</sup> who, in fact, succeeded to trap dimethylsilylene in hydrocarbon glasses at 77 K and in an Ar matrix at 10 K, and observed its ultraviolet, visible, and infrared spectra. A number of kinetic studies have been performed on dimethylsilylene; two recent time-resolved investigations are mentioned here. Baggott et al.<sup>125)</sup> generated  $(\text{CH}_3)_2\text{Si}$  by the photolysis of pentamethyldisilane at 193 nm and measured the rate constants of the reactions  $(\text{CH}_3)_2\text{Si} + \text{SiH}_4$  and its four methyl derivatives by monitoring the transient absorption of  $(\text{CH}_3)_2\text{Si}$  at 457.9 nm. Shizuka et al.<sup>126)</sup> also observed the transient absorption of  $(\text{CH}_3)_2\text{Si}$  at 470 nm by the laser photolysis of dodecamethylcyclohexasilane dissolved in methylcyclohexane; the lifetime of dimethylsilylene was found to be about 200 ns at 293 K. Drahnak et al.<sup>127)</sup> found that  $(\text{CH}_3)_2\text{Si}$  was converted to methylmethylenesilane  $\text{CH}_2=\text{SiHCH}_3$  by irradiation with 450-nm light, and that the latter

was converted back to the former by 248-nm light. A few *ab initio* calculations have been performed, yielding structural parameters. Grev and Schaefer<sup>128)</sup> estimated the torsional frequencies to be 55 and 124 cm<sup>-1</sup> for the con- and counter-rotation of the two methyl groups, respectively. Gordon<sup>129)</sup> calculated the permanent dipole moment to be about 1.2 D ( $4.0 \times 10^{-30}$  C m).

Because dimethylsilylene has been known to act as a key intermediate in many reactions of organometallic compounds, Fujitake and Hirota<sup>130)</sup> have attempted to observe its microwave spectrum, which, when observed, will be useful in diagnosing the mechanisms of gas-phase reactions in real time. They employed five methods to generate dimethylsilylene: (1) the pyrolysis of 1,2-dimethoxy-1,1,2,2-tetramethyldisilane, (2) a mercury-sensitized reaction of dodecamethylcyclohexasilane, (3) a discharge in tetramethylsilane, (4) the excimer-laser photolysis of dodecamethylcyclohexasilane and phenyldimethylsilane, and finally (5) a reaction of dimethyldichlorosilane with sodium vapor. They scanned a few frequency regions between 320 to 360 GHz for each of the five cases and observed some absorption lines of a transient species in cases (2) and (5), but could not obtain any assignment. It is also worth trying to observe the laser-induced fluorescence spectrum of (CH<sub>3</sub>)<sub>2</sub>Si in the gaseous phase, which, if observed at high resolution, would provide a clue for assigning the rotational spectrum.

The author is grateful to the following people for collaboration: C. Yamada, M. Fujitake, K. Kawaguchi, T. Ishiwata, I. Tanaka, N. Ohashi, T. Goto, N. Itabashi, N. Nishiwaki, S. Naito, M. Magane, H. Nomura, H. Kanamori, Y. Kawashima, Y. Endo, T. Suzuki, S. Tsuchiya, and M. Okunishi.

## References

- 1) S. G. Lias, J. E. Bartmess, J. F. Liebman, J. L. Holmes, R. D. Levin, and W. G. Mallard, *J. Phys. Chem. Ref. Data*, **17**, Suppl. 1 (1988).
- 2) A. V. Nemukhin, J. Almlöf, and A. Heiberg, *Chem. Phys.*, **57**, 197 (1981).
- 3) J. R. Woodward, J. S. Hayden, and J. L. Gole, *Chem. Phys.*, **134**, 395 (1989).
- 4) R. R. Herm and D. R. Herschbach, *J. Chem. Phys.*, **52**, 5783 (1970).
- 5) S. M. Freund, E. Herbst, R. P. Mariella, Jr., and W. Klemperer, *J. Chem. Phys.*, **56**, 1467 (1972).
- 6) D. M. Lindsay, D. R. Herschbach, and A. L. Kwiram, *J. Chem. Phys.*, **60**, 315 (1974).
- 7) C. Yamada, M. Fujitake, and E. Hirota, *J. Chem. Phys.*, **90**, 3033 (1989).
- 8) C. Yamada, M. Fujitake, and E. Hirota, *J. Chem. Phys.*, **91**, 137 (1989).
- 9) C. Yamada and E. Hirota, *J. Chem. Phys.*, **99**, 8489 (1993).
- 10) H. W. Sarkas, J. H. Hendricks, S. T. Arnold, V. L. Slager, and K. H. Bowen, *J. Chem. Phys.*, **100**, 3358 (1994).
- 11) P. A. G. O'Hare and A. C. Wahl, *J. Chem. Phys.*, **56**, 4516 (1972).
- 12) M. Yoshimine, *J. Chem. Phys.*, **57**, 1108 (1972).
- 13) D. T. Grow and R. M. Pitzer, *J. Chem. Phys.*, **67**, 4019 (1977).
- 14) J. N. Allison and W. A. Goddard, III, *J. Chem. Phys.*, **77**, 4259 (1982).
- 15) J. N. Allison, R. J. Cave, and W. A. Goddard, III, *J. Phys. Chem.*, **88**, 1262 (1984).
- 16) S. R. Langhoff, C. W. Bauschlicher, Jr., and H. Partridge, *J. Chem. Phys.*, **84**, 4474 (1986).
- 17) E. P. F. Lee, T. G. Wright, and J. M. Dyke, *Mol. Phys.*, **77**, 501 (1992).
- 18) R. F. Curl, P. G. Carrick, and A. J. Merer, *J. Chem. Phys.*, **82**, 3479 (1985); **83**, 4278 (1985).
- 19) M. Guélin and P. Thaddeus, *Astrophys. J.*, **212**, L81 (1977); C. A. Gottlieb, E. W. Gottlieb, P. Thaddeus, and H. Kawamura, *Astrophys. J.*, **275**, 916 (1983).
- 20) S. Yamamoto, S. Saito, M. Guélin, J. Chernicharo, H. Suzuki, and M. Ohishi, *Astrophys. J.*, **323**, L149 (1987).
- 21) H. Suzuki, M. Ohishi, N. Kaifu, S. Ishikawa, T. Kasuga, S. Saito, and K. Kawaguchi, *Publ. Astron. Soc. Jpn.*, **38**, 911 (1986).
- 22) S. Saito, K. Kawaguchi, H. Suzuki, M. Ohishi, N. Kaifu, and S. Ishikawa, *Publ. Astron. Soc. Jpn.*, **39**, 193 (1987).
- 23) C. Amiot and J. Verges, *Chem. Phys. Lett.*, **95**, 189 (1983).
- 24) C. Yamada, E. Hirota, S. Yamamoto, and S. Saito, *J. Chem. Phys.*, **88**, 46 (1988).
- 25) C. W. Bauschlicher, Jr., H. Partridge, and K. G. Dyall, *Chem. Phys. Lett.*, **199**, 225 (1992).
- 26) S. Chapman, *Astrophys. J.*, **90**, 309 (1939).
- 27) J. M. C. Plane and D. Husain, *J. Chem. Soc., Faraday Trans. 2*, **82**, 2047 (1986).
- 28) D. R. Herschbach, C. E. Kolb, D. R. Worsnop, and X. Shi, *Nature*, **356**, 414 (1992).
- 29) J. Cederberg, D. Olson, P. Soulen, K. Urberg, H. Ton, T. Steinbach, B. Mock, K. Jarausch, P. Haertel, and M. Bresnahan, *J. Mol. Spectrosc.*, **154**, 43 (1992).
- 30) C. D. Hollowell, A. T. Hebert, and K. Street, Jr., *J. Chem. Phys.*, **41**, 3540 (1964).
- 31) C. Yamada, S. Yamamoto, and E. Hirota, unpublished.
- 32) C. Yamada and E. Hirota, to be published.
- 33) C. D. Hollowell and F. Lange, *Z. Naturforsch.*, **A**, **29a**, 1548 (1974).
- 34) H. G. Bannwitz, R. Haerten, O. Klais, and G. Müller, *Chem. Phys. Lett.*, **9**, 19 (1971).
- 35) R. P. Wayne, I. Barnes, P. Biggs, J. P. Burrows, C. E. Canosa-Mas, J. Hjorth, G. Le Bras, G. K. Moortgat, D. Perner, G. Poulet, G. Restelli, and H. Sidebottom, "The Nitrate Radical: Physics, Chemistry, and the Atmosphere 1990," in "Air Pollution Report 31," Commission of the European Communities, 1990.
- 36) T. Ishiwata, I. Fujiwara, Y. Naruge, K. Obi, and I. Tanaka, *J. Phys. Chem.*, **87**, 1349 (1983).
- 37) H. H. Nelson, L. Pasternack, and J. R. McDonald, *J. Phys. Chem.*, **87**, 1286 (1983).
- 38) B. Kim, P. L. Hunter, and H. S. Johnston, *J. Chem. Phys.*, **96**, 4057 (1992).
- 39) B. J. Howard, (private communication)

- 40) B. Kim and H. Katô, (private communication)
- 41) A. D. Walsh, *J. Chem. Soc.*, **1953**, 2301.
- 42) A. Weaver, D. W. Arnold, S. E. Bradforth, and D. M. Neumark, *J. Chem. Phys.*, **94**, 1740 (1991).
- 43) T. E. H. Walker and J. A. Horsley, *Mol. Phys.*, **21**, 939 (1971).
- 44) P. E. M. Siegbahn, *J. Comput. Chem.*, **6**, 182 (1985).
- 45) B. Kim, H. S. Johnston, D. A. Clabo, Jr., and H. F. Schaefer, III, *J. Chem. Phys.*, **88**, 3204 (1988).
- 46) R. D. Davy and H. F. Schaefer, III, *J. Chem. Phys.*, **91**, 4410 (1989).
- 47) R. C. Boehm and L. L. Lohr, *J. Phys. Chem.*, **93**, 3430 (1989).
- 48) U. Kaldor, *Chem. Phys. Lett.*, **166**, 599 (1990).
- 49) B. Kim, B. L. Hammond, W. A. Lester, Jr., and H. S. Johnston, *Chem. Phys. Lett.*, **168**, 131 (1990).
- 50) V. R. Morris, S. C. Bhatia, and J. H. Hall, Jr., *J. Phys. Chem.*, **94**, 7414 (1990).
- 51) U. Kaldor, *Chem. Phys. Lett.*, **185**, 131 (1991).
- 52) J. F. Stanton, J. Gauss, and R. J. Bartlett, *J. Chem. Phys.*, **94**, 4084 (1991).
- 53) T. Ishiwata, I. Tanaka, K. Kawaguchi, and E. Hirota, *J. Chem. Phys.*, **82**, 2196 (1985).
- 54) K. Kawaguchi, E. Hirota, T. Ishiwata, and I. Tanaka, *J. Chem. Phys.*, **93**, 951 (1990).
- 55) E. Hirota, K. Kawaguchi, T. Ishiwata, and I. Tanaka, *J. Chem. Phys.*, **95**, 771 (1991).
- 56) R. R. Friedl and S. P. Sander, *J. Phys. Chem.*, **91**, 2721 (1987).
- 57) K. Kawaguchi, T. Ishiwata, I. Tanaka, and E. Hirota, *Chem. Phys. Lett.*, **180**, 436 (1991).
- 58) T. Ishiwata, I. Tanaka, K. Kawaguchi, and E. Hirota, *J. Mol. Spectrosc.*, **153**, 167 (1992).
- 59) M. Mayer, L. S. Cederbaum, and H. Köppel, *J. Chem. Phys.*, **100**, 899 (1994).
- 60) T. Ishiwata, K. Kawaguchi, M. Fujitake, N. Ohashi, I. Tanaka, and E. Hirota, unpublished.
- 61) E. Hirota, unpublished.
- 62) C. Yamada and E. Hirota, *Phys. Rev. Lett.*, **56**, 923 (1986).
- 63) C. Yamada, E. Hirota, and K. Kawaguchi, *J. Chem. Phys.*, **75**, 5256 (1981).
- 64) For example: Y. Ellinger, F. Pauzat, V. Barone, J. Douady, and R. Subra, *J. Chem. Phys.*, **72**, 6390 (1980).
- 65) R. D. Johnosn, III, B. P. Tsai, and J. W. Hudgens, *J. Chem. Phys.*, **91**, 3340 (1989).
- 66) N. Itabashi, K. Kato, N. Nishiwaki, T. Goto, C. Yamada, and E. Hirota, *Jpn. J. Appl. Phys.*, **27**, L1565 (1988).
- 67) N. Itabashi, K. Kato, N. Nishiwaki, T. Goto, C. Yamada, and E. Hirota, *Jpn. J. Appl. Phys.*, **28**, L325 (1989).
- 68) N. Itabashi, N. Nishiwaki, M. Magane, S. Naito, T. Goto, A. Matsuda, C. Yamada, and E. Hirota, *Jpn. J. Appl. Phys.*, **29**, L505 (1990).
- 69) N. Itabashi, N. Nishiwaki, M. Magane, T. Goto, A. Matsuda, C. Yamada, and E. Hirota, *Jpn. J. Appl. Phys.*, **29**, 585 (1990).
- 70) Y. Sumiyoshi, K. Tanaka, and T. Tanaka, *Appl. Surf. Sci.*, **79/80**, 471 (1994).
- 71) I. Dubois, G. Herzberg, and R. D. Verma, *J. Chem. Phys.*, **47**, 4262 (1967).
- 72) I. Dubois, *Can. J. Phys.*, **46**, 2485 (1968).
- 73) I. Dubois, G. Duxbury, and R. N. Dixon, *J. Chem. Soc., Faraday Trans. 2*, **71**, 799 (1975).
- 74) H. Ishikawa and O. Kajimoto, *J. Mol. Spectrosc.*, **150**, 610 (1991).
- 75) H. Ishikawa and O. Kajimoto, *J. Mol. Spectrosc.*, **160**, 1 (1992).
- 76) M. Fukushima, S. Mayama, and K. Obi, *J. Chem. Phys.*, **96**, 44 (1992).
- 77) M. Fukushima and K. Obi, *J. Chem. Phys.*, **100**, 6221 (1994).
- 78) C. Yamada, H. Kanamori, E. Hirota, N. Nishiwaki, N. Itabashi, K. Kato, and T. Goto, *J. Chem. Phys.*, **91**, 4582 (1989).
- 79) C. Yamada, M. Okunishi, E. Hirota, N. Nishiwaki, N. Itabashi, H. Nomura, and T. Goto, unpublished.
- 80) A. R. W. McKellar, P. R. Bunker, T. J. Sears, K. M. Evenson, R. J. Saykally, and S. R. Langoff, *J. Chem. Phys.*, **79**, 5251 (1983).
- 81) For example: K. Balasubramanian and A. D. McLean, *J. Chem. Phys.*, **85**, 5117 (1986).
- 82) M. Bogey, H. Bolvin, C. Demuynck, and J. L. Destombes, *Phys. Rev. Lett.*, **66**, 413 (1991).
- 83) M. Bogey, H. Bolvin, M. Cordonnier, C. Demuynck, J. L. Destombes, and A. G. Császár, *J. Chem. Phys.*, **100**, 8614 (1994).
- 84) M. Cordonnier, M. Bogey, C. Demuynck, and J. L. Destombes, *J. Chem. Phys.*, **97**, 7984 (1992).
- 85) P. B. Davies and P. M. Martineau, *J. Chem. Phys.*, **88**, 485 (1988).
- 86) D. M. Smith, P. M. Martineau, and P. B. Davies, *J. Chem. Phys.*, **96**, 1741 (1992).
- 87) P. B. Davies and D. M. Smith, *J. Chem. Phys.*, **100**, 6166 (1994).
- 88) E. J. Goodwin, N. W. Howard, and A. C. Legon, *Chem. Phys. Lett.*, **131**, 319 (1986).
- 89) N. W. Howard and A. C. Legon, *J. Chem. Phys.*, **88**, 4694 (1988).
- 90) Y. Kawashima, C. Yamada, and E. Hirota, *J. Chem. Phys.*, **94**, 7707 (1991).
- 91) Y. Kawashima and E. Hirota, *J. Chem. Phys.*, **96**, 2460 (1992).
- 92) Y. Kawashima and E. Hirota, *J. Mol. Spectrosc.*, **153**, 466 (1992).
- 93) E. Hirota and Y. Kawashima, to be published.
- 94) M. Uemura, (private communication).
- 95) E. Hirota, *J. Mol. Spectrosc.*, **153**, 447 (1992).
- 96) Y. Kawashima and E. Hirota, unpublished.
- 97) A. G. Maki and R. L. Sams, *J. Chem. Phys.*, **75**, 4178 (1981).
- 98) K. Kawaguchi, M. Ohishi, S. Ishikawa, and N. Kaifu, *Astrophys. J.*, **386**, L51 (1992).
- 99) K. Kawaguchi, S. Takano, M. Ohishi, S. Ishikawa, K. Miyazawa, N. Kaifu, K. Yamashita, S. Yamamoto, S. Saito, Y. Ohshima, and Y. Endo, *Astrophys. J.*, **396**, L49 (1992).
- 100) K. Kawaguchi, Y. Kasai, S. Ishikawa, M. Ohishi, N. Kaifu, and T. Amano, *Astrophys. J.*, **420**, L95 (1994).
- 101) *Ab initio* values calculated by S. Green and E. Herbst, *Astrophys. J.*, **229**, 121 (1979).
- 102) C. Yamada and E. Hirota, unpublished.
- 103) Y. Xie and J. E. Boggs, *J. Chem. Phys.*, **90**, 4320 (1989).



- 104) T. J. Lee, A. Willetts, J. F. Graw, and N. C. Handy, *J. Chem. Phys.*, **90**, 4330 (1989).
- 105) N. C. Craig, J. Pranata, S. J. Reinganum, J. R. Sprague, and P. S. Stevens, *J. Am. Chem. Soc.*, **108**, 4378 (1986).
- 106) H. Kanamori, Y. Endo, and E. Hirota, in "Dynamics of Excited Molecules," ed by K. Kuchitsu, Elsevier, Amsterdam (1993), Chap. 2, pp. 9—54.
- 107) Y. Endo, H. Kanamori, and E. Hirota, *Laser Chem.*, **7**, 61 (1987).
- 108) T. Suzuki, H. Kanamori, and E. Hirota, *J. Chem. Phys.*, **94**, 6607 (1991).
- 109) R. J. Buss, R. J. Baseman, G. He, and Y. T. Lee, *J. Photochem.*, **17**, 389 (1981).
- 110) Y. Endo, S. Tsuchiya, C. Yamada, E. Hirota, and S. Koda, *J. Chem. Phys.*, **85**, 4446 (1986).
- 111) A. M. Schmoltner, P. M. Chu, R. J. Brudzynski, and Y. T. Lee, *J. Chem. Phys.*, **91**, 6926 (1989).
- 112) E. Hirota, C. Yamada, and M. Okunishi, *J. Chem. Phys.*, **97**, 2963 (1992).
- 113) C. L. Currie and D. A. Ramsay, *J. Chem. Phys.*, **45**, 488 (1966).
- 114) A. B. Callear and H. K. Lee, *Trans. Faraday Soc.*, **64**, 308 (1968).
- 115) H. C. Longuet-Higgins and E. W. Abrahamson, *J. Am. Chem. Soc.*, **87**, 2045 (1965).
- 116) See also : S. Olivella, A. Solé, and J. M. Bofill, *J. Am. Chem. Soc.*, **112**, 2160 (1990).
- 117) J. D. Getty, M. J. Burmeister, S. G. Westre, and P. B. Kelly, *J. Am. Chem. Soc.*, **113**, 801 (1991).
- 118) K. Holtzhauser, C. Cometta-Morini, and J. F. M. Oth, *J. Phys. Org. Chem.*, **3**, 219 (1990).
- 119) S. Olivella, (private communication).
- 120) M. Okunishi and E. Hirota, unpublished.
- 121) K. U. Ingold, (private communication).
- 122) J. A. Blush, D. W. Minsek, and P. Chen, *J. Phys. Chem.*, **96**, 10150 (1992).
- 123) M. Ishikawa and M. Kumada, *J. Organomet. Chem.*, **42**, 325 (1972).
- 124) T. J. Drahnak, J. Michl, and R. West, *J. Am. Chem. Soc.*, **101**, 5427 (1979).
- 125) J. E. Baggott, M. A. Blitz, H. M. Frey, P. D. Lightfoot, and R. Walsh, *Chem. Phys. Lett.*, **135**, 39 (1987).
- 126) H. Shizuka, H. Tanaka, K. Tonokura, K. Murata, H. Hiratsuka, H. Ohshita, and M. Ishikawa, *Chem. Phys. Lett.*, **143**, 225 (1988).
- 127) T. J. Drahnak, J. Michl, and R. West, *J. Am. Chem. Soc.*, **103**, 1845 (1981).
- 128) R. S. Grev and H. F. Schaefer, III, *J. Am. Chem. Soc.*, **108**, 5804 (1986).
- 129) M. S. Gordon, (private communication).
- 130) M. Fujitake and E. Hirota, unpublished.



- 1958 Research Associate at the Department of Chemistry, Faculty of Science, The University of Tokyo.
- 1959 Ph D.
- 1960—1962 Research Fellow at the Department of Chemistry, Harvard University.
- 1962 Lecturer of the Department of Chemistry, Faculty of Science, The University of Tokyo.
- 1964 Associate Professor of the Department of Chemistry, Faculty of Science, The University of Tokyo.
- 1968 Professor of the Department of Chemistry, Faculty of Science, Kyushu University.
- 1975 Professor of the Institute for Molecular Science.
- 1990 Vice President of the Graduate University for Advanced Studies.